ORIGINAL ARTICLE

Interfacial Morphology and Bonding Mechanism of Explosive Weld Joints

Tingting Zhang[1,2], Wenxian Wang[3*], Zhifeng Yan[3] and Jie Zhang[3]

Abstract

Interfacial structure greatly affects the mechanical properties of laminated plates. However, the critical material properties that impact the interfacial morphology, appearance, and associated bonding mechanism of explosive welded plates are still unknown. In this paper, the same base plate (AZ31B alloy) and different flyer metals (aluminum alloy, copper, and stainless steel) were used to investigate interfacial morphology and structure. SEM and TEM results showed that typical sine wave, wave-like, and half-wave-like interfaces were found at the bonding interfaces of Al/Mg, Cu/Mg and SS/Mg clad plates, respectively. The different interfacial morphologies were mainly due to the differences in hardness and yield strength between the flyer and base metals. The results of the microstructural distribution at the bonding interface indicated metallurgical bonding, instead of the commonly believed solid-state bonding, in the explosive welded clad plate. In addition, the shear strength of the bonding interface of the explosive welded Al/Mg, Cu/Mg and SS/Mg clad plates can reach up to 201.2 MPa, 147.8 MPa, and 128.4 MPa, respectively. The proposed research provides the design basis for laminated composite metal plates fabrication by explosive welding technology.

Keywords: Interfacial structure, Bonding mechanism, Explosive welding, Metallurgical bonding, Magnesium alloy

1 Introduction

Alloys of magnesium (Mg), the lightest structural metal, show promise in important value applications in the automotive, aerospace and other industries that require economical energy consumption and environmental friendliness [1, 2]. However, the application of Mg is restricted by its poor corrosion and wear resistance properties [3]. Therefore, Mg-based laminated composites, which are fabricated by cladding corrosion-resistant metals (such as stainless steel [SS], copper alloy [Cu] and aluminum alloy [Al]), would be promising materials to meet these requirements due to their excellent overall performance. Thus, developing a welding process to fabricate Mg-based composite materials is essential.

Various methods have been explored to join the dissimilar metals of Mg-based composite materials. Butt and overlap joints of Mg-based composites have been

created by diffusion welding [4–6], arc welding [7–9], spot welding [10, 11], friction stir welding [12, 13], and rolling processes [14–16]. However, some problems are encountered in the dissimilar welding of Mg alloys and other metals, which are mainly caused by the marked differences in the metallurgical and physical properties between the dissimilar metals. One issue is the formation of excessive intermetallic compounds (e.g., with Mg-Cu joints and Mg-Al joints) or almost no intersolubility at the interface (e.g., with Mg-Ti joints and Mg-steel joints), leading to a poor joint. Explosive welding is well known for its capability of directly joining various dissimilar metals that cannot be bonded through traditional welding processes [17]. This technology is also suitable for fabricating large-scale composite laminates. During explosive welding, a flyer plate with an inclined angle impacts the base plate, and a joint of dissimilar materials is obtained. A schematic "weldability window" was developed by Blazynski in 1987 that defines the conditions to achieve desirable welds [18]. Trykow et al. [19] was one of the first to attempt to fabricate Al/Mg composite plates by explosive welding.

*Correspondence: wangwenxian@tyut.edu.cn
[3] College of Materials Science and Engineering, Taiyuan University of Technology, Taiyuan 030024, China
Full list of author information is available at the end of the article

Zhang *et al. Chin. J. Mech. Eng.* (2021) 34:8

Page 2 of 12

However, they found that the Mg alloys were not suitable for direct joining with Al alloys. Yan et al. [20] and Chen et al. [21] investigated the microstructure and mechanical properties of an Mg/Al explosive welded composite plate. They found by scanning electron microscopy (SEM) analysis that a local diffusion layer was formed at the bonding interface. The influence of heat treatment on an Al/Mg explosive welded composite plate was investigated by Zhang et al. [22]. Greenberg et al. [23] found that a local metallic was formed in Cu/Ta explosive welded joints. However, the bonding mechanism and its influencing factors at the whole interface along the explosive welding direction are still ambiguous, especially for a composite plate with a base plate comprising a Mg alloy.

It is generally believed that a wavy interface is a key factor for good joint formation during explosive welding. However, with the variety of different combinations of materials, some new interfacial shapes and structures are presented. The Cu/Al interface was extensively studied under explosive welding processes, and it was found that an interfacial morphology with a straight bond zone indicates a sufficiently consistently bonded Cu/Al explosive weld. Loureiro et al. [24] investigated the influence of the explosive ratio and type of sensitizer on the quality of Cu/Al explosive welded clad. They found intermittent molten pockets instead of a sine-shaped wavy interface that comprised brittle Al-Cu intermetallic phases. Gulenc [25] studied the effect of the explosive ratio on the interfacial morphologies of aluminum and copper plates by explosive welding. He found that the interface was transformed from linear to wavy and its wavelength and amplitude increased with the increasing explosive ratio. Athar et al. [26] investigated an Al/Cu/Al laminated plate fabricated by explosive welding. They found that different morphologies (straight, wavy and melted) for the welding interface formed with the changing welding parameters. Additionally, Carvalho et al. [26] investigated the effect of flyer material on interfacial morphology, and they found that physical properties directly affect the formation of the wavy interface, in addition to factors that influence the welding parameters. Therefore, it is essential to investigate the interfacial morphologies and bonding mechanism at the bonding interface after explosive welding between different flyer metals (stainless steel, copper alloy and aluminum alloy) and the same base plate (Mg alloy).

This research aims to investigate the relationship between the interfacial morphology and the bonding mechanism during explosive welding. Experiments were performed using the same base plate comprising an AZ31B Mg alloy and different flyer plates: 304 stainless steel (304SS), H68 Cu alloy and AA6061 Al alloy.

2 Experimental Procedures

2.1 Experimental Parameters

The installation diagram of the explosive welding process is illustrated in Figure 1. A parallel configuration between the flyer plate and the base plate was used, as illustrated in Figure 1a. A series of three explosive welding experiments were performed with the same base metal plate (AZ31B magnesium alloy). Before welding, a certain amount of explosives was put on the flyer plate by using paper boxes. The flyer metals were 304 stainless steel (304SS), H68 Cu alloy and AA6061 Al alloy. All flyer plates were prepared with dimensions of 650 mm× 350 mm× 2 mm, and the base plate had dimensions of 600 mm × 300 mm × 15 mm. During the explosive welding process, using a flyer plate that is slightly larger than the base plate can increase the bonding area. To remove coarse contaminants from the contact surfaces, all plates were ground with sand papers up to 400 grades. In order to present the explosive welding process, a schematic of the explosive welding experiment was shown in Figure 1b. An explosive charge was uniformly placed on the surface of the flyer plate with a detonator at its edge. The distance gaps of equal height were placed vertically between the flyer plate and base plate. An ammonium nitrate explosive and diesel fuel oil (ANFO) powder mix was used, and its density was approximately 0.7 g/cm^3. ANFO is a low-velocity explosive with a velocity of approximately 2500 m/s. The explosive welding parameters are shown in Table 1.

2.2 Measurement and Characterization Techniques

To investigate the interfacial morphologies, samples that included the bonding interface were cut from the central part of the clad plate in a direction parallel to the detonation direction. The samples were prepared using standard metallographic techniques and finally polished with a 0.06 μm colloidal silica suspension to remove the deformation zone. A Hitachi S3400N scanning electron microscope equipped with an Oxford Instruments energy dispersive spectrometer (EDS) and electron backscattered diffraction (EBSD) system was used to characterize the microstructural evolution near the interface. The EBSD maps and grain orientations for the microstructural characterization were analyzed using the Oxford HKL Channel 5 software package. Transmission electron microscopy (TEM) analyses were conducted with a JEOL-2100 instrument equipped with an EDS operating at 200 kV to determine the interfacial bonding mechanism and microstructure in the melted interlayer zone. The TEM specimens were prepared using a TASCAN focused ion beam (FIB) system and were sliced along the direction perpendicular to the bonding interface. To characterize the interfacial bonding strength of the
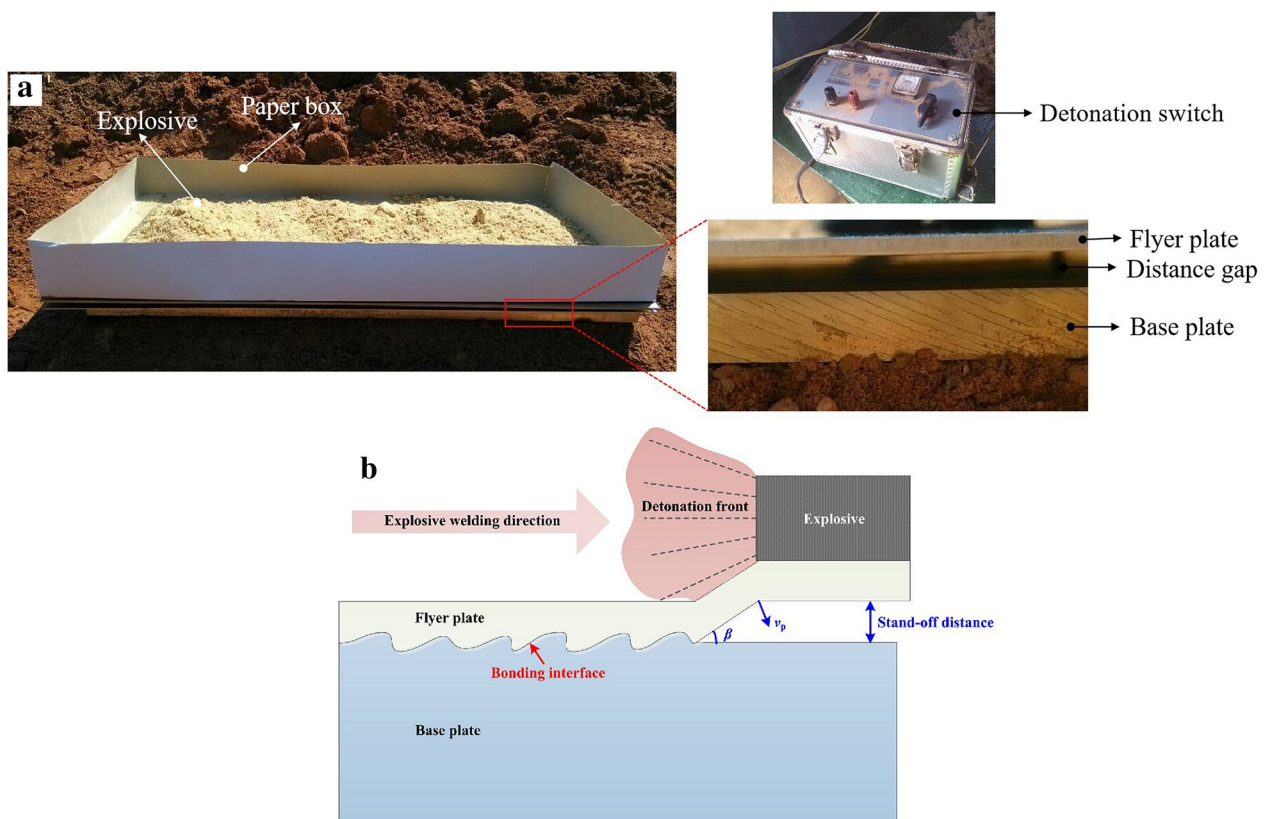
Zhang *et al. Chin. J. Mech. Eng.* (2021) 34:8

Page 3 of 12

Figure 1 Installation diagrams of the explosive welding process

Table 1 Welding parameters of the bimetal combinations used in the experiments

Materials	Thickness of explosive (mm)	Stand-off distance (mm)
AA6061/AZ31B	20	3
	20	6
H68/AZ31B	20	5
304SS/AZ31B	20	5

explosive welded plates, a pressure-shear test was carried out. For shear strength tests, specimens with dimensions of 6 mm × 8 mm × 4 mm were cut that included the bonding interface, and a specially designed testing fixture was used. The shear strength test was conducted in a ZWICKZ020 materials testing system at a shearing speed of 1 mm/min.
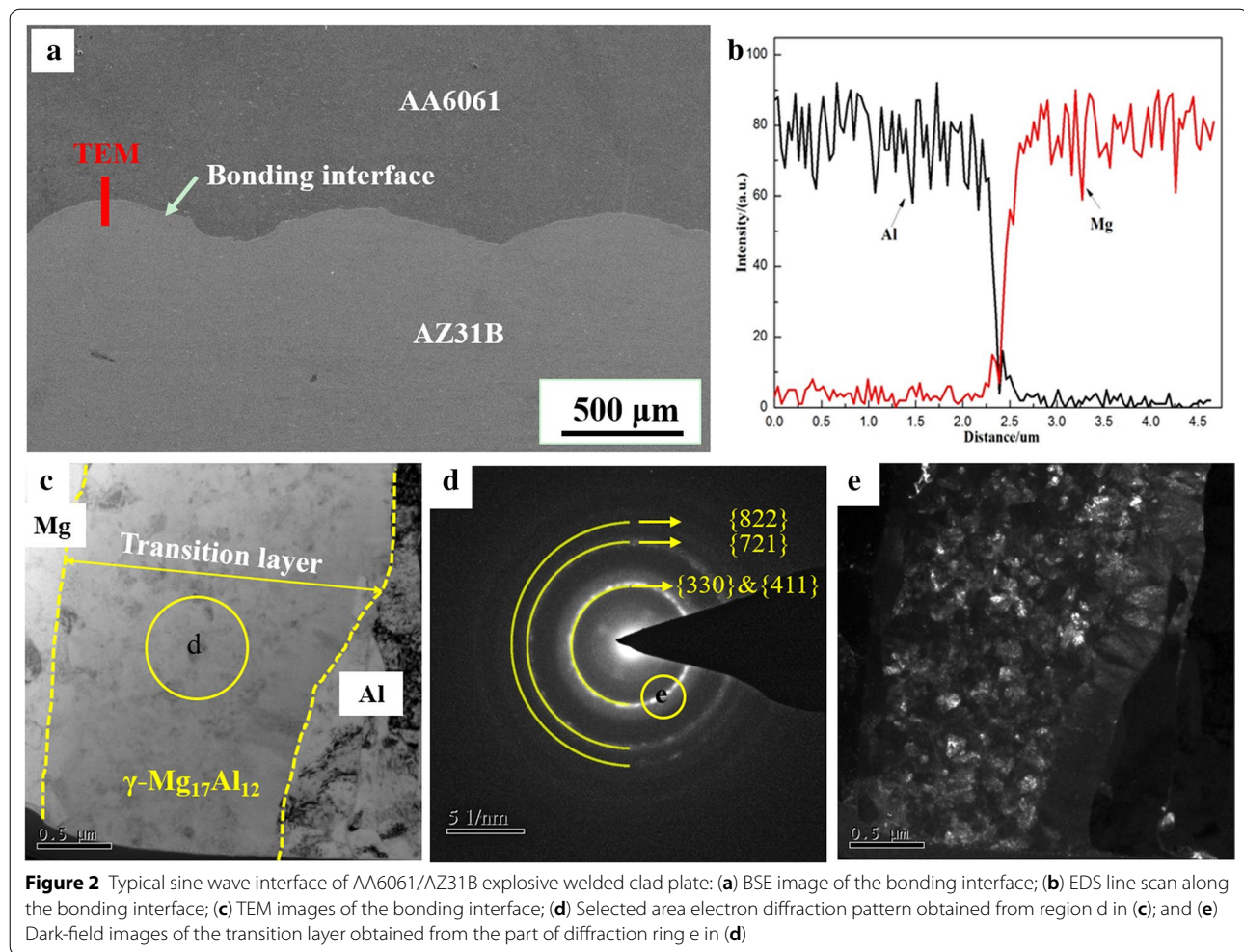
3 Results
3.1 Explosive Welding of Al Alloy to Mg Alloy
AA6061 Al/AZ31B Mg clad plates were successfully fabricated by an explosive welding process. The morphology

and microstructure of the bonding interface were revealed by the EBSD and TEM techniques. During the explosive welding, different welding stand-off distances (3 mm and 6 mm, as displayed in Table 1) were used; the bonding interfaces are shown in Figures 2 and 3, respectively.

The interfaces shown in Figure 2 and Figure 3 show similar interfacial bonding shapes. As the backscattered electron (BSE) images at the bonding interface show, the AA6061/AZ31B clad plate presents a morphology similar to a sine wave, as illustrated in Figures 2a and 3a. However, there are some typical differences. The amplitude and wavelength are different, and a local melted zone with a vortex structure was found, as marked by the dashed white arrow. To analyze the interfacial bonding, a line scan of the Al and Mg was conducted using EDS. The results in Figure 2b show that the thickness of the transition layer was less than 2 μm, making it difficult to clearly observe the bonding mechanism.

To further investigate the microstructure at the interface of Al/Mg alloy, TEM testing was carried out, and a TEM sample consisting of a bonding interface was prepared using the FIB technique. Figure 2c shows the microstructure at the bonding interface obtained with
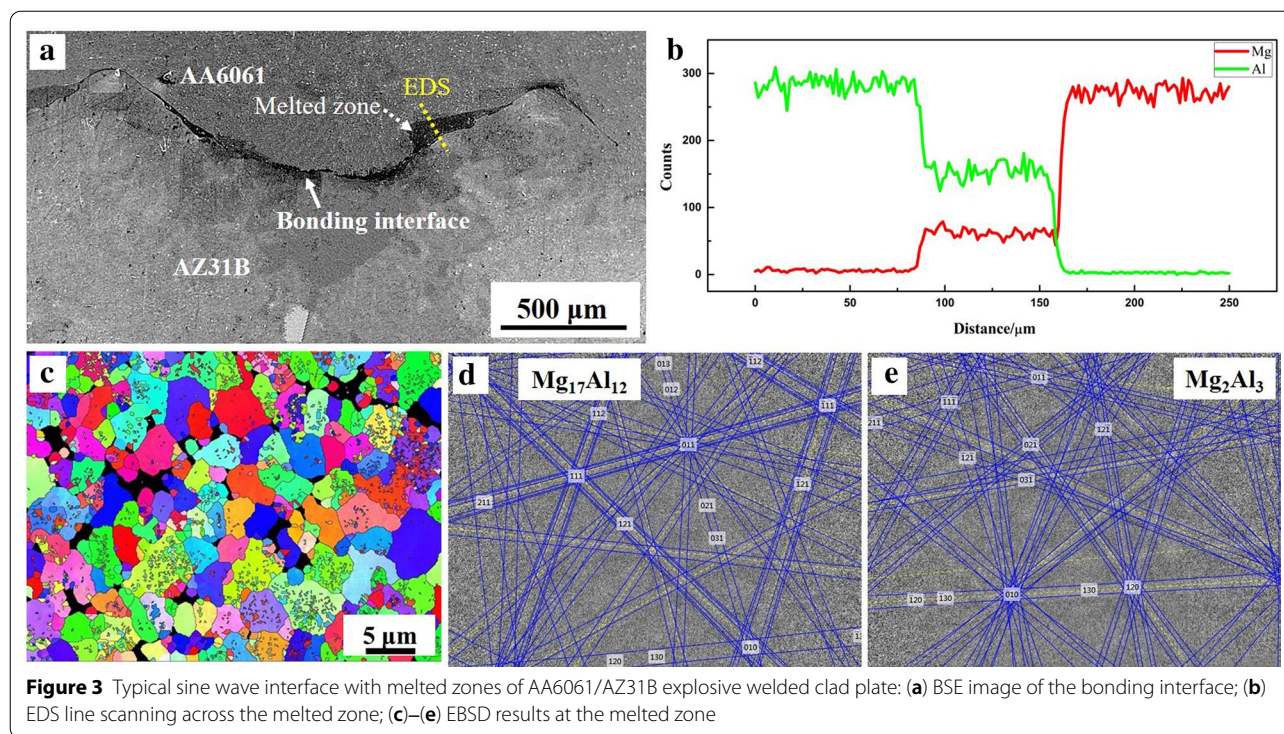
Figure 2 Typical sine wave interface of AA6061/AZ31B explosive welded clad plate: (**a**) BSE image of the bonding interface; (**b**) EDS line scan along the bonding interface; (**c**) TEM images of the bonding interface; (**d**) Selected area electron diffraction pattern obtained from region d in (**c**); and (**e**) Dark-field images of the transition layer obtained from the part of diffraction ring e in (**d**)

TEM, and a new γ-$Mg_{17}Al_{12}$ phase can be observed. In Figure 2d, the SAED pattern could be indexed as a polycrystalline $Mg_{17}Al_{12}$ phase, and the corresponding planes were marked. The formation of the inner brightest diffraction ring is due to the superimposed {330} and {411} diffraction planes, where the diffraction indexes are summed. In the outer diffraction {330} and {411} ring, a wide diffuse diffraction ring could be observed, which may be due to the superimposed {322}, {422} and {510} diffraction planes. The dark-field image of the bonding interface in Figure 2e also provides direct evidence for the polycrystalline nature of the $Mg_{17}Al_{12}$ phase. Therefore, nano-$Mg_{17}Al_{12}$ grains were formed at the interface after explosive welding. The formation of the γ-$Mg_{17}Al_{12}$ phase at the transition layer can be explained by a locally high temperature distribution near the interface that is much higher than the melting points of the AA6061 and AZ31B metals [27].

As shown in Figure 3, the bonding interface of AA6061/AZ31B presents a sine wave shape with vortexes, where

the vortexes are local melted zones. The formation of a vortex structure may be due to the large plastic deformation and the local high temperature distribution at the interface caused by the larger stand-off distance during the explosive welding. The sine wave interface can be explained by the movement of the jets and the plastic deformation of both the flyer plate and base plate. The formation of a metallic jet is essential to clean the surfaces and guarantee a strong bond between experimental metals. During the explosive welding, most of the jets travelled forward; however, a small portion changed direction and swirled back due to the large plastic deformation and continually penetrated the flyer plate to form a vortex. To investigate the distribution of elements across the vortex structure at the bonding interface, an EDS line scan of Al and Mg was obtained.

In order to analyze the microstructure in the melted zone at the interface of Al/Mg alloy, both EBSD and EDS techniques were adopted to study. The results were shown in Figure 3b–d. As shown in Figure 3b, a mixed

Figure 3 Typical sine wave interface with melted zones of AA6061/AZ31B explosive welded clad plate: (**a**) BSE image of the bonding interface; (**b**) EDS line scanning across the melted zone; (**c**)–(**e**) EBSD results at the melted zone

intermetallic compound zone, containing Al and Mg, formed in the melted zone. The microstructure in the melted zone was further characterized by EBSD, and the results are shown in Figure 3c–e. Fine grains ($Mg_{17}Al_{12}$ and Mg_2Al_3 phases) were formed in the melted zone. Comparing Figure 2 to 3, a higher impact velocity with the flyer plate will occur when a larger stand-off distance between the flyer plate and base plate is adopted, and this change will lead to a higher temperature distribution and larger plastic deformation near the interface compared to those with a small stand-off distance. In the explosive welding process, the temperature rise near the interface should be high enough to melt materials and lead to the formation of a melted zone [28]. Therefore, it can be concluded that a melted transition layer formed along the whole interface, except for at the vortexes, which guarantees the formation of a metallurgical joint between the AA6061 flyer plate and the AZ31B base plate after the explosive welding process.

3.2 Explosive Welding of Cu Alloy to Mg Alloy
In this study, an H68 Cu/AZ31B Mg alloy clad plate was fabricated by explosive welding. The results of the SEM and TEM characterizations at the bonding interface are presented in this section.

A typical BSE image of the interface at the cross section of the H68/AZ31B explosive welded clad plate is shown in Figure 4a. It is shown that an irregularly shaped

joint was formed, and this joint is just a wave-like interface compared to the bonding interface of the AA6061/AZ31B explosive welded clad plate. The EDS line scan of the Cu, Zn and Mg element distribution across the transition layer, denoted by the dashed yellow arrow line, is shown in Figure 4b. It is evident that the mixing zone includes Cu and Zn, which came from the H68 flyer metal, and Mg, which came from the AZ31B base metal. The mixing zone was formed at the joint, and the thickness of the transition layer was approximately 20 μm.

To further analyze the microstructure at the joint, a TEM analysis was carried out, where the TEM sample was prepared perpendicular to the interface (marked by the yellow line and shown in Figure 4a) using the FIB technique. The results show that the joint consists of a diffusion layer near the Cu matrix (marked by the white dotted line zone in Figure 4c) and a melted zone, which is consistent with the result shown in Figure 4b. In the melted zone, brighter $CuZn_2$ phases can be inferred from the selected area diffraction pattern results (as illustrated in Figure 4e and f). The results confirm that the primitive cubic $CuZn_2$ phase with a cell parameter of 7.761 Å and the crystal axis $[\bar{2}\ \bar{3}\ 12]$ was present. The formation of a diffusion layer and melted layer can be reasonably explained by the local high temperature at the interface [29]. Therefore, it can be concluded that a metallurgic joint was formed between the H68 flyer plate and the AZ31B base plate after the explosive welding process; the
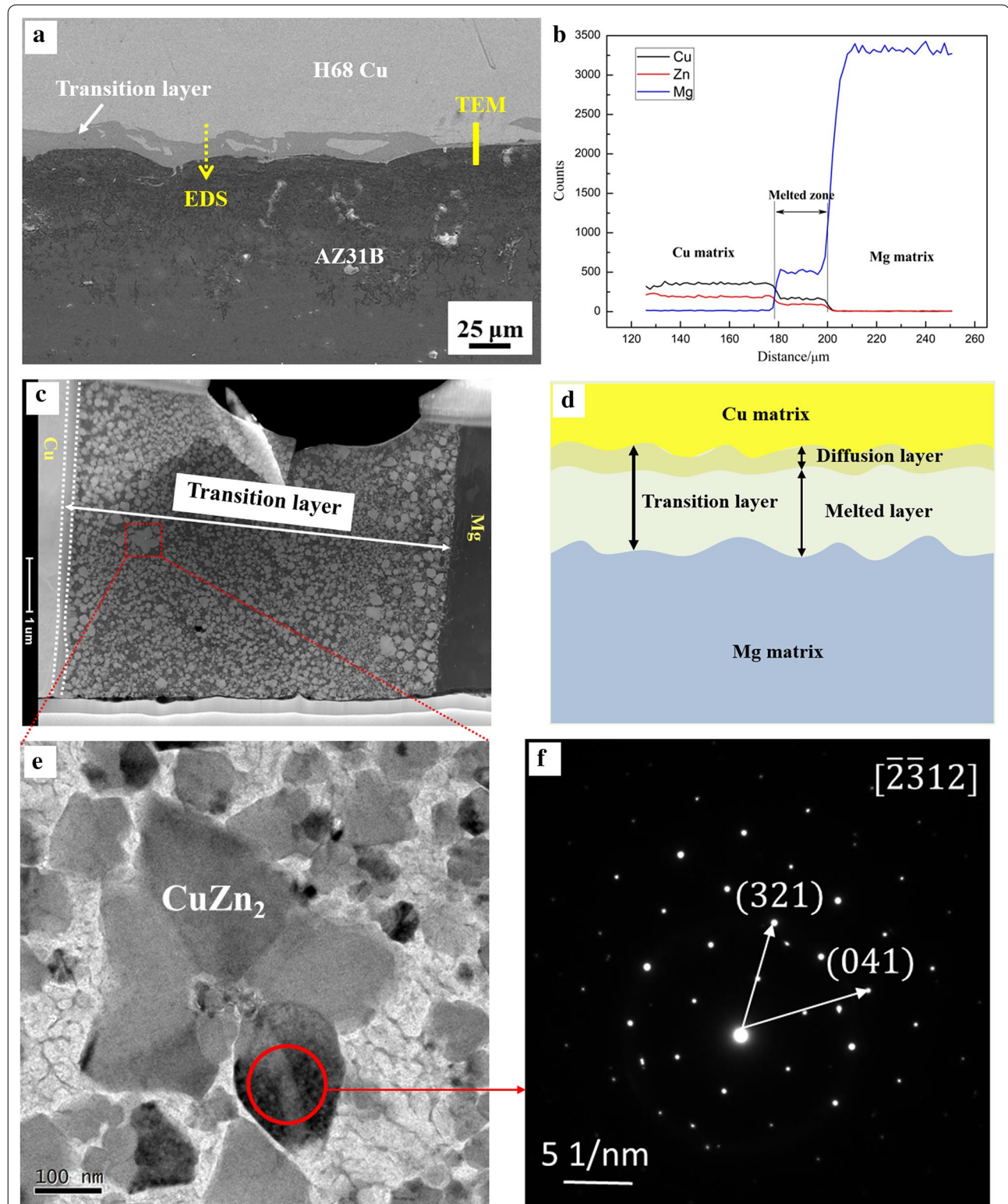
Zhang *et al. Chin. J. Mech. Eng.* (2021) 34:8

Page 6 of 12

Figure 4 The wave-like interface of the H68/AZ31B explosive welded clad plate: (**a**) BSE image of the bonding interface; (**b**) EDS line scanning obtained perpendicular to the bonding interface; (**c**) TEM images at the transition layer; (**d**) Typical structures at the bonding interface; (**e**) Enlarged view of new phase zone (Red dashed box shown in (**c**)); (**f**) Selected area electron diffraction pattern image

joint can be described as a typical structure, as shown in the schematic in Figure 4d.

3.3 Explosive Welding of Steel to Mg Alloy

The composite materials of magnesium alloys and austenitic steels can potentially be applied in many automotive and aerospace components [29, 30]. A 304SS/AZ31B Mg alloy clad plate was fabricated by explosive welding. In this section, the results of SEM and TEM/EDS characterizations at the bonding interface are presented.

Figure 5 shows the cross-section morphology and microstructure of the 304SS/AZ31B alloy clad plate after the explosive welding. As shown in Figure 5a, the bonding interface exhibited a "half-wave-like" morphology with an obvious transition layer, compared to that in Figures 2a, 3a and 4a. To further analyze the bonding mechanism of the 304SS/AZ31B welded joint, the microstructure at this transition layer was characterized by SEM and TEM. As shown in the enlarged BSE image of the transition layer in Figure 5b (marked by the red cross-shaped zone in Figure 5a), it is evident that many white particles were distributed throughout the dark Mg matrix. The chemical composition of the white particles, as shown in Figure 5b, can be identified by TEM. The TEM results at the transition layer interface further confirmed that the (Fe, Cr, Al)-rich particles are spherical, as indicated by the red arrows in Figure 5c. TEM/EDS line scanning analysis results across the interface of the 304SS and transition layer are illustrated in Figure 5d.

At the 304SS/transition layer interface, a thin diffusion layer was formed at the interface after explosive welding. As shown in Figure 5d, Mg from the AZ31B Mg alloy matrix was the major chemical component in the transition layer, except for some (Fe, Cr, Al)-rich particles. Therefore, the metallurgic joint consists of a thin diffusion layer and a melted layer after explosive welding, and this transition layer guarantees effective bonding between the 304SS metal plate and the AZ31B metal plate, as presented in Figure 5e.

3.4 Interfacial Bonding Strength

The interfacial bonding strength of the explosive welded clad plate was determined through pressure-shear strength tests. The load-displacement curves of the bonding interface of all clad plates are shown in Figure 6.

As shown in Figure 6, the maximum loads during the pressure-shear testing are 6030.0 N, 6438.4 N, 4730.0 N and 4110.0 N for the AA6061/AZ31B cladding plates with the wavy interface and wavy interface with vortex, H68/AZ31B and 304SS/AZ31B, respectively. The optimum interfacial bonding shear strengths of the Al/Mg, Cu/Mg and SS/Mg explosive welded clad plate were calculated to be 201.2 MPa, 147.8 MPa and 128.4 MPa,

respectively. A higher bonding strength can be obtained for the AA6061/AZ31B clad plate with a wavy interface with a vortex compared to that without the vortex because the vortex can increase the bonding area at the interface between the flyer plate and base plate.
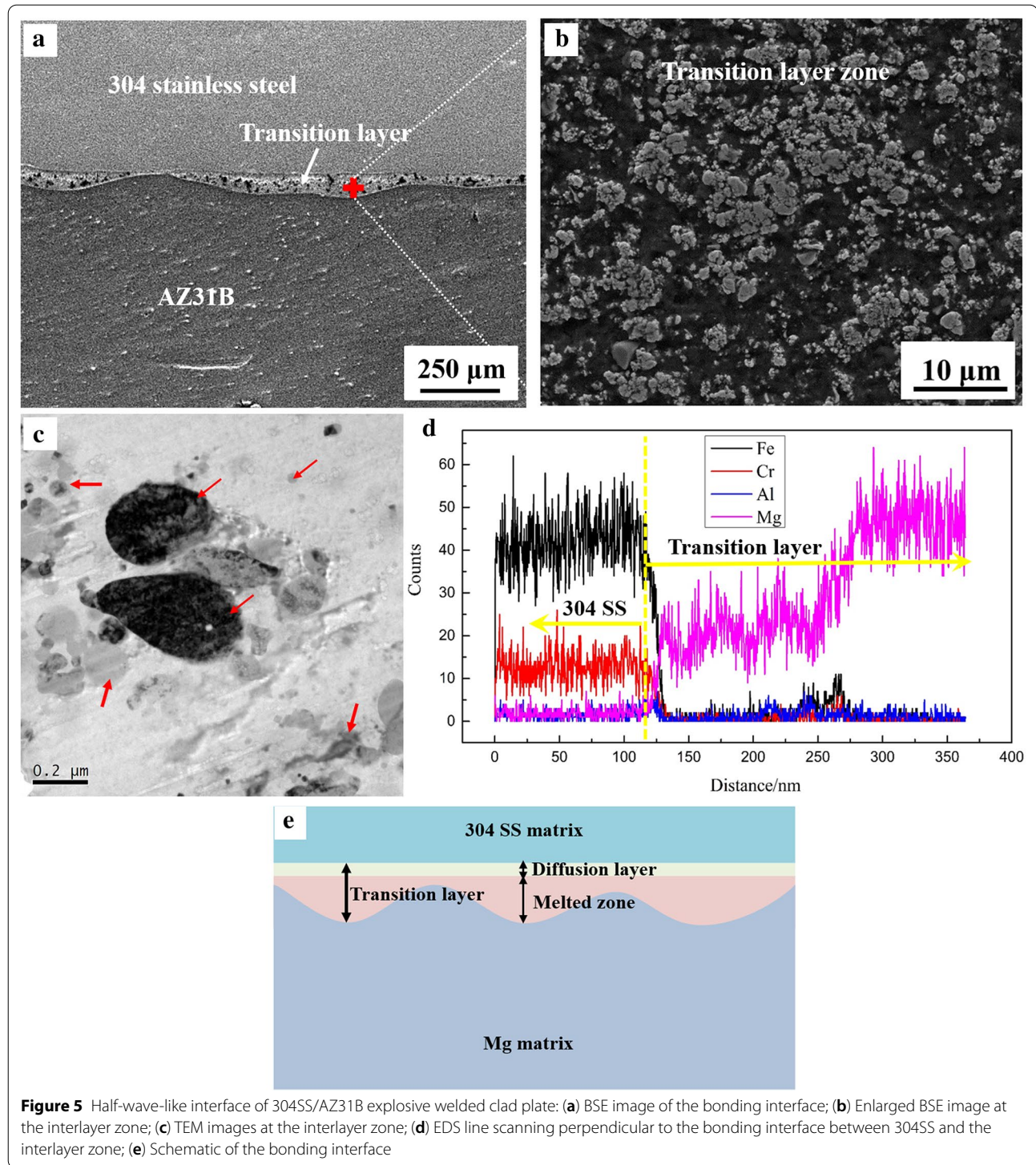
4 Discussion

To investigate the influence of the physical and mechanical properties of the metal on the interfacial morphology, the experimental results of the bonding interface and related material properties are presented in Table 2.

4.1 Interfacial Morphologies of the Clad Plates

Three different flyer metals impacted the same base metal plate. Earlier researches [31–33] have been proved that the typical wavy interface is controlled and formed by the periodic oscillation in the jet flow at the collision zone between the flyer and base plate. However, during the collision zone, the deformation degree and interfacial morphologies at the interface were different after explosive welding for different materials and welding parameters. In addition, the pressure produced at the collision point due to the action of jet must be of sufficient magnitude to exceed the dynamic elastic limit of the material. As the earlier researches, the density and hardness of the metals also affect the interfacial morphology during explosive welding. This phenomenon is mainly caused by the different contributions of the jets from the flyer and base plates [34].
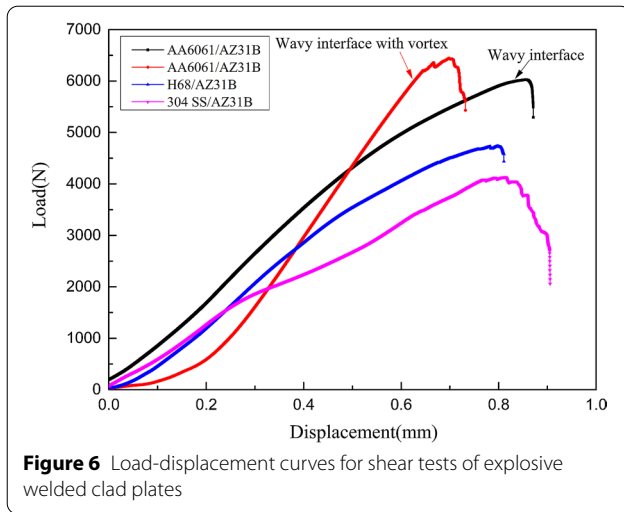
According to the boundary conditions of the weldability window, which is mainly related to the phenomena occurring at the interface, each line represents a limit that is related to a specific phenomenon [35]. Among the lines in the weldability window, the condition related to a wavy interface is the impact velocity (v_p), wherein the resulting impact pressure exceeded the yield stress of the materials [36]. Thus, the interfacial morphology is related to the yield strength of the experimental metals during the explosive welding. As shown in Table 2, the yield strength of the AZ31B Mg alloy is only slightly lower than that of AA6061 but significantly lower than those of H68 and 304SS. The plastic deformation distinctly decreased when the yield strength of the flyer plates increased, thereby leading to the formation of different interfacial morphologies. Hence, plastic deformation at the collision can be easily accommodated when the yield strength values of the flyer and base metals are close.

Therefore, under the same action of periodic oscillation in the jet flow, the interfacial morphologies and wavy size were mainly depend on the yield strength. There are almost in agreement with the yield strength value between AA6061 and AZ31B alloy plate, and then the coordinated plastic deformation are much easier to

Figure 5 Half-wave-like interface of 304SS/AZ31B explosive welded clad plate: (**a**) BSE image of the bonding interface; (**b**) Enlarged BSE image at the interlayer zone; (**c**) TEM images at the interlayer zone; (**d**) EDS line scanning perpendicular to the bonding interface between 304SS and the interlayer zone; (**e**) Schematic of the bonding interface

occur at the bonding interface. So a typical wavy interface can form for Al/Mg cladding plate. For Cu/Mg interface, the lower yield strength of Mg alloy than that of Cu (as shown in Table 2), uncoordinated deformation (a smaller plastic deformation for Cu interfacial side and

a large wavy deformation for Mg alloy interfacial side) was occurred. So the "wave-like" interfacial morphology formed for Cu/Mg cladding plate. Similarly, the yield strength value of Mg alloy is far lower than that of 304SS, so an flat interface (almost undeformed) was keep at the

Zhang *et al. Chin. J. Mech. Eng.* (2021) 34:8

Page 9 of 12

Figure 6 Load-displacement curves for shear tests of explosive welded clad plates

Figure 7 Simplified schematic of the temperature distribution at the collision zone during explosive welding

304SS interface side, while a large wavy deformation for Mg alloy interfacial side) was occurred during explosive welding. Therefore, a "half-wave-like" shape interface was formed at the SS/Mg interface.

4.2 Temperature Distribution at the Interface

Investigating the temperature variation in the collision zone is crucial to understanding the interfacial bonding mechanism. The temperature distribution, theory, and specific values are not discussed herein, but the major characteristics can be highlighted to understand the differences in the bonding interface, considering that the clad plates had the same base metal. A highly localized temperature zone was formed at the front of the collision point during explosive welding. In addition, the temperature of the metals surrounding the collision point increased because the pressure and the plastic deformation between the flyer plate and base plate increased. This temperature was high enough to melt the metals in the collision zone (schematically shown in Figure 7). This phenomenon was also found in simulation results and theoretical prediction of explosive welding joints [29, 33,
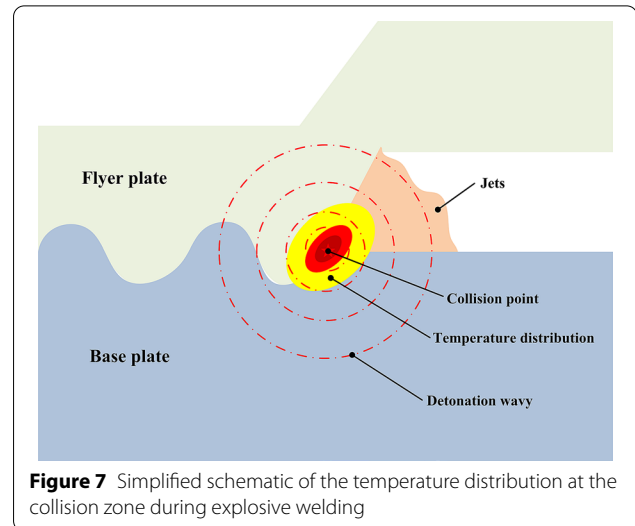
37, 38]. All the results presented that the interfacial temperature was able to reach 10^4 K or even 10^5 K, which is well above the melting point of almost of metals.

In this study, the melting points of the AA6061 flyer plate and the AZ31B base plate are close. Therefore, their contributions to the molten metal at the bonding interface zone are similar, and this can also be used to explain the formation of the $Mg_{17}Al_{12}$ intermetallic compounds. The melting points of the H68 Cu and 304SS flyer plates were considerably higher than that of the AZ31B base plate. Hence, much more Mg alloy matrix could be melted at the collision zone. This molten AZ31B alloy (α-Mg) immediately filled the gap that was formed by the uncoordinated deformation at the collision zone. Therefore, the mixture at the bonding interface was mainly from the AZ31B base plate. However, the temperature starts to decrease when the collision point moves forward due to heat exchange with the environment and heat transfer to the less heated adjacent zone. Thus, in the transition layer zone, the mixed molten metals quickly solidified, and a metallurgic joint was then formed.

Table 2 Interfacial morphologies and experimental physical and mechanical properties of Al/Mg, Cu/Mg and SS/Mg explosive welds

Clad plate	Interfacial morphology	Metals	Physical properties		Mechanical properties (Room temperature)		
			Density (g/cm^3)	Melting point (℃)	Hardness (HV)	Tensile strength (MPa)	Yield strength (MPa)
AA6061/AZ31B	Sine wave	AZ31B	1.74	630	68	238	152
AA6061/AZ31B	Sine wave (vortex)	AA6061	2.7	660	82	285	160
H68Cu/AZ31B	Wave-like	H68	8.5	1193	115	236	202
304SS/AZ31B	Half-wave-like	304SS	7.93	1440	220	520	260

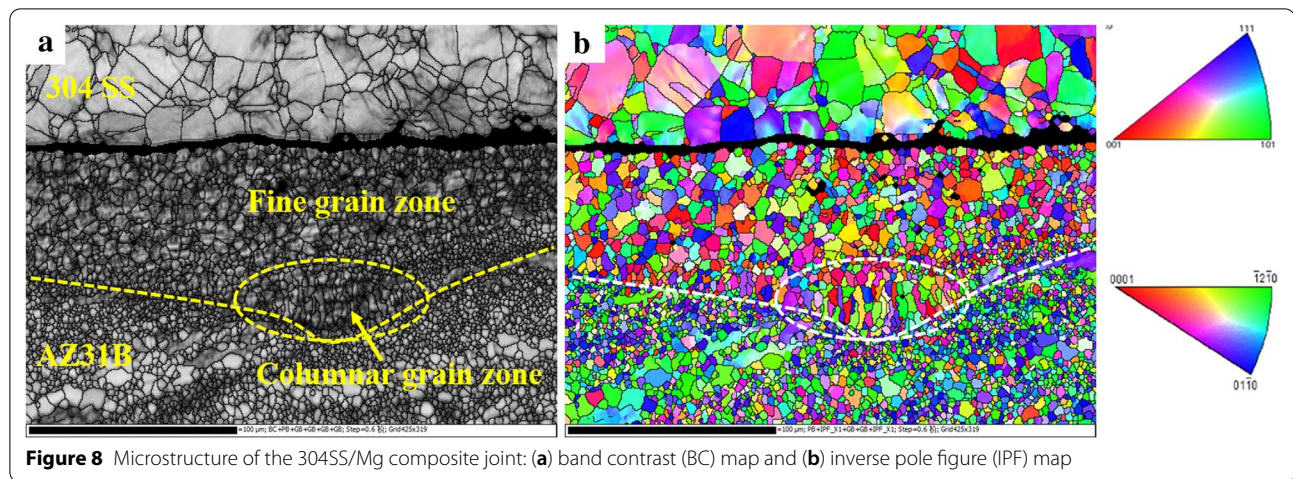Zhang *et al. Chin. J. Mech. Eng.* (2021) 34:8

Page 10 of 12

Figure 8 Microstructure of the 304SS/Mg composite joint: (**a**) band contrast (BC) map and (**b**) inverse pole figure (IPF) map

4.3 Metallurgic Bonding Mechanism at the Interface

According to the microstructure and temperature distribution results at the interface of Mg-based clad plate after explosive welding, both local metal melting especially Mg alloy metal near the interface and the formation of new intermetallic compounds or other phases (γ-$Mg_{17}Al_{12}$, Mg_2Al_3, molten α-Mg, $CuZn_2$ and (Fe, Cr, Al)-rich) were occurred in the Al/Mg, Cu/Mg, and SS/Mg clad plates. So these results confirmed that a metallurgic bonding during explosive welding was formed for Mg-based metal clad plate.

Other direct proof of the metallurgical bonding caused by melting at a high temperature can be obtained from the microstructure characteristics, as shown in Figure 8. Both the band contrast (BC) map and the inverse pole figure (IPF) map in Figure 8 indicate that the joint consists of columnar grains at the bottom and fine grains at the center in the interlayer zone of the 304SS/Mg composite plate. The microstructure at the 304SS/Mg explosive welded joint was similar to that in a typical fusion weld pool. This phenomenon can be attributed to the cooling rate being considerably higher at the bottom adjacent to the original AZ31B base plate than at the center of the joint. Thus, columnar crystals appeared at the bottom, whereas fine equiaxed grains formed at the center of the interlayer zone. During explosive welding, elemental diffusion also occurred at the interface between the flyer plate and the transition layer under high temperature and pressure conditions. However, only a thin diffusion layer was formed because the time was extremely short for diffusion. Therefore, the bonding mechanism of the bonding interface was due to metallurgical bonding caused by the melted zone at high temperatures near the interface, instead of the commonly believed solid-state bonding.

5 Conclusions

(1) The SEM and TEM images of the bonding interface in the explosive welded Mg-based clad plate illustrated that typical sine wave, wave-like, and half-wave-like interfaces were obtained in the Al/Mg, Cu/Mg, and SS/Mg clad plates, respectively.

(2) The interfacial morphology of the explosive welding was strongly influenced by the physical and mechanical properties of both the flyer metal and base metal. The uncoordinated deformation degree was obvious in the collision zone, with greater differences in the hardness and yield strength between the flyer plate and base plate.

(3) A solidified transition interlayer was formed, and the flyer plate was bonded to the base plate during explosive welding. A thin diffusion layer also appeared at the bonding interface during the explosive welding process.

(4) The bonding mechanism of the bonding interface was due to metallurgical bonding caused by melting and diffusion at high temperature near the interface in the explosive welded cladding plate.

(5) The shear strengths of the bonding interfaces of the explosive welded Al/Mg, Cu/Mg and SS/Mg clad plates can reach up to 201.2 MPa, 147.8 MPa and 128.4 MPa, respectively.

Zhang *et al. Chin. J. Mech. Eng.* (2021) 34:8

Page 11 of 12

Authors' Information

Tingting Zhang, born in 1988, is currently a post-doctoral research at *College of Mechanical and Vehicle Engineering, Taiyuan University of Technology, China*. She received her PhD degree from *Taiyuan University of Technology, China*, in 2017. Her research interests include composite fabrication and interfacial behavior research.

Wenxian Wang, born in 1963, is currently a professor at *Taiyuan University of Technology, China*. He received his PhD degree from *Tianjin University, China*, in 2002.

Zhifeng Yan, born in 1984, is currently an associate professor at *Taiyuan University of Technology, China*. He received his PhD degree from *Taiyuan University of Technology, China*, in 2014.

Jie Zhang, born in 1996, is currently a master candidate at *Taiyuan University of Technology, China*.

Author Details

[1] Advanced Forming and Intelligent Equipment Research Institute, Taiyuan University of Technology, Taiyuan 030024, China. [2] College of Mechanical and Vehicle Engineering, Taiyuan University of Technology, Taiyuan 030024, China. [3] College of Materials Science and Engineering, Taiyuan University of Technology, Taiyuan 030024, China.

References

[1]   W Heike, K Christina, U Madlen, et al. Determination of the hot cracking tendency of a twin-roll cast AZ31 magnesium alloy by means of gleeble tests. *Materials Science Forum*, 2018, 918: 40-47.

[2]   S Kumar, S K Das. Characterization of mechanical properties and nano-porous structure of Aluminium-Magnesium alloy during multi-axial tensile deformation: An atomistic investigation. *Journal of Alloys & Compounds*, 2018, 740: 626-638.

[3]   C Ma, G Peng, L Nie, et al. Laser surface modification of Mg-Gd-Ca alloy for corrosion resistance and biocompatibility enhancement. *Applied Surface Science*, 2018, 445: 211-216.

[4]   A Azizi, H Alimardan. Effect of welding temperature and duration on properties of 7075 Al to AZ31B Mg diffusion bonded joint. *Transactions of Nonferrous Metals Society of China*, 2016, 26(1): 85-92.

[5]   F Yin, C Liu, Y Zhang, et al. Effect of Ni interlayer on characteristics of diffusion bonded Mg/Al joints. *Materials Science and Technology*, 2018, 34(9): 1-8.

[6]   S Du, G Liu, M Wang. Diffusion bonding preparation of AZ31B/Cu composite and analysis of interface microstructure. *Rare Metal Materials & Engineering*, 2014, 43(2): 475-480.

[7]   R Cao, J H Chang, Q Huang, et al. Behaviors and effects of Zn coating on welding-brazing process of Al-Steel and Mg-steel dissimilar metals. *Journal of Manufacturing Processes*, 2018, 31: 674-688.

[8]   G Song, J Yu, T Li, et al. Effect of laser-GTAW hybrid welding heat input on the performance of Mg/Steel butt joint. *Journal of Manufacturing Processes*, 2018, 31: 131-138.

[9]   G Song, H Y Wang, T T Li, et al. Joining mechanism of Mg alloy/steel butt joints with Cu-Zn interlayer by hybrid laser-TIG welding source. *Journal of Iron & Steel Research International*, 2018, 25(2): 221-227.

[10]   Q Cui, Y LI, J Yang, et al. Effects of chemical plating Sn coating on the ultrasonic spot welding of Mg/Al dissimilar metals. *Materials Science & Technology*, 2017, 25(2): 35-38.

[11]   D Ren, L Liu. Interface microstructure and mechanical properties of arc spot welding Mg-steel dissimilar joint with Cu interlayer. *Materials & Design*, 2014, 59(7): 369-376.

[12]   Y S Sato, S H C Park, M Michiuchi, et al. Constitutional liquation during dissimilar friction stir welding of Al and Mg alloys. *Scripta Materialia*, 2004, 50(9): 1233-1236.

[13]   J Verma, R V Taiwade, C Reddy, et al. Effect of friction stir welding process parameters on Mg-AZ31B/Al-AA6061 joints. *Materials & Manufacturing Processes*, 2017, 33(3): 308-314.

[14]   K Tanaka, H T Takeshita, K Kurumatani, et al. The effect of initial structures of Mg/Cu super-laminates on hydrogen absorption/desorption properties. *Journal of Alloys & Compounds*, 2013, 580(24): S222-S225.

[15]   A L Wei, X H Liu, L Dong, et al. Binding property of Al/Mg/Al thin plates fabricated by one-pass hot rolling with different reduction ratios, temperatures and annealing treatments. *Rare Metals*, 2018, 2: 1-7.

[16]   M Abbasi, S A Sajjadi. Mechanical properties and interface evaluation of Al/AZ31 multilayer composites produced by ARB at different rolling temperatures. *Journal of Materials Engineering & Performance*, 2018, 27(7): 1-13.

[17]   K Raghukandan, K Hokamoto, P Manikandan, et al. Optimization of process parameters in explosive cladding of mild steel and aluminum. *Metals & Materials International*, 2004, 10(2): 193-197.

[18]   T Z Blazynski. *Explosive welding, forming and compaction*. First ed. Applied Science Publishers Barking, Essex, England, 1987.

[19]   Y P Trykov, V G Shmorgun, V D Rogozin, et al. Technology of explosive welding magnesium-aluminium composite joints. *Welding International*, 2003, 17(8): 661-664.

[20]   Y B Yan, Z W Zhang, W Shen, et al. Microstructure and properties of magnesium AZ31B-aluminum 7075 explosively welded composite plate. *Materials Science & Engineering: A*, 2010, 527(9): 2241-2245.

[21]   P Chen, J Feng, Q Zhou. Investigation on the explosive welding of 1100 aluminum alloy and AZ31 magnesium alloy. *Journal of Materials Engineering and Performance*, 2016, 25(7): 2635-2641.

[22]   N Zhang, W Wang, X Cao, et al. The effect of annealing on the interface microstructure and mechanical characteristics of AZ31B/AA6061 composite plates fabricated by explosive welding. *Materials & Design*, 2015, 65: 1100-1109.

[23]   B A Greenberg, M A Ivanov, A V Inozemtsev, et al. Microheterogeneous structure of local melted zones in the process of explosive welding. *Metallurgical and Materials Transactions A*, 2015, 46(8): 3569-3580.

[24]   A Loureiro, R Mendes, J B Ribeiro, et al. Effect of explosive mixture on quality of explosive welds of copper to aluminum. *Materials & Design*, 2016, 95(5): 256-267.

[25]   B Gulenc. Investigation of interface properties and weldability of aluminum and copper plates by explosive welding method. *Materials & Design*, 2008, 29(1): 275-278.

[26]   M M H Athar, B Tolaminejad. Weldability window and the effect of interface morphology on the properties of Al/Cu/Al laminated composites fabricated by explosive welding. *Materials & Design*, 2015, 86: 516-525.

[27]   T T Zhang, W X Wang, W Zhang, et al. Microstructure evolution and mechanical properties of an AA6061/AZ31B alloy plate fabricated by explosive welding. *Journal of Alloys & Compounds*, 2018, 735: 1759-1768.

[28]   A Durgutlu, H Okuyucu and B Gulenc. Investigation of effect of the stand-off distance on interface characteristics of explosively welded copper and stainless steel. *Materials and Design*, 2008, 29(7): 1480-1484.

[29]   I A Bataev, D V Lazurenko, S Tanaka. High cooling rates and metastable phases at the interfaces of explosively welded materials. *Acta Materialia*, 2017, 135: 277-289.

[30]   E Ratte, S Leonhardt, W Bleck, et al. Energy absorption behaviour of austenitic and duplex stainless steels in a crash box geometry. *Steel Research International*, 2006, 77(9-10): 692-697.

Zhang *et al. Chin. J. Mech. Eng.* (2021) 34:8

Page 12 of 12

[31] Q Chu, M Zhang, J Li. Experimental and numerical investigation of microstructure and mechanical behavior of titanium/steel interfaces prepared by explosive welding. *Materials Science & Engineering A*, 2017, 689: 323-331.

[32] T T Zhang, W X Wang, W Zhang, et al. Interfacial microstructure evolution and deformation mechanism in an explosively welded Al/Mg alloy plate. *Journal of Materials Science*, 2019, 54: 9155-9167.

[33] X Yuan, W Wang, X Cao, et al. Numerical study on the interfacial behavior of Mg/Al plate in explosive/impact welding. *Science & Engineering of Composite Materials*, 2015, 24(4): 581-590.

[34] W D Rosset. Analysis of explosive bonding parameters. *Advanced Manufacturing Processes*, 2006, 21(6): 634-638.

[35] W Elthalabawy, T Khan. Liquid phase bonding of 316L stainless steel to AZ31 magnesium alloy. *Journal of Materials Science & Technology*, 2011, 27(1): 22-28.

[36] G H S F L Carvalho, R Mendes, R M Leal, et al. Effect of the flyer material on the interface phenomena in aluminium and copper explosive welds. *Materials & Design*, 2017, 122: 172-183.

[37] H Hampel, U Richter. Formation of interface waves in dependence of the explosive welding parameters. *Acta Mechanica Sinaca*, 1989, 5: 97-102.

[38] S C Han. *Phase transformation and fractography of interface of explosive welding*. Beijing: National Defence Industry Press, 2011.